



Published in final edited form as:

Nat Chem Biol. 2014 August ; 10(8): 626–628. doi:10.1038/nchembio.1551.

DrugTargetSeqR: a genomics- and CRISPR/Cas9-based method to analyze drug targets

Corynn Kasap, Olivier Elemento, and Tarun M. Kapoor*

Abstract

To identify the physiological targets of drugs and bioactive small molecules we have developed an approach, named DrugTargetSeqR, which combines high-throughput sequencing, computational mutation discovery and CRISPR/Cas9-based genome editing. We apply this approach to isipinesib and YM155, drugs that have undergone clinical trials as anti-cancer agents, and demonstrate target identification and uncover genetic and epigenetic mechanisms likely to cause drug resistance in human cancer cells.

Deconvolving the mechanisms of action of chemical inhibitors is a major challenge in drug discovery and chemical biology research^{1, 2}. When the target of a drug is not known, it is difficult to improve its efficacy or reduce any unanticipated toxicity, and its use as a probe for studying cellular mechanisms is restricted. Therefore, several approaches have been developed to identify the targets of bioactive chemicals^{1, 2}. Recently, pooled shRNA-based knockdown and CRISPR/Cas9-mediated gene deletion-methods have been developed to unravel the mechanisms of action of chemical inhibitors and toxic agents^{3–5}. A major limitation of these approaches is that determining if a candidate protein is the drug's physiological target depends on correlations between protein knockdown and pharmacological inhibition phenotypes. These correlations often fail due to differences between cellular responses to fast-acting (typically, minutes) chemical inhibitors and the cumulative direct and indirect effects of protein knockdown, which can require significant time (typically, hours)⁶.

High confidence in establishing a protein as a drug's direct target is achieved when a mutation in the protein confers resistance to the chemical inhibitor in cells and also suppresses drug activity in a biochemical assay, e.g., drug-binding or kinase assay⁷. To achieve this 'gold standard' (or 'genetic') proof of a drug's target we have developed an approach that uses next-generation sequencing-based discovery of high frequency drug-resistance conferring mutations in human cancer cells⁷. Our findings suggest that resistance

Users may view, print, copy, and download text and data-mine the content in such documents, for the purposes of academic research, subject always to the full Conditions of use:http://www.nature.com/authors/editorial_policies/license.html#terms

Correspondence: Kapoor@rockefeller.edu, The Rockefeller University, 1230 York Avenue, New York, NY10065, (212) 327 -8176.

Contributions:

CK carried out all experiments except cDNA library preparation and sequencing as detailed in Methods. OE conducted bioinformatics analysis. TMK and OE directed experiments. TMK, OE, and CK wrote the manuscript.

Competing financial interests:

We declare that the authors have no competing interests as defined by Nature Publishing Group, or other interests that might be perceived to influence the results and discussion reported in this paper.

via mutations in the drug's direct target arises at frequencies sufficient for our approach to be effective in human cells that have large complex genomes⁸. However, testing whether any single mutation can confer drug resistance in human cells typically involves transgene overexpression and may fail for several reasons, such as toxicity. We reasoned that direct genome editing would circumvent this major obstacle and developed an integrated approach for drug target identification. This method, which we name DrugTargetSeqR, (with 'Seq' for transcriptome sequencing and 'R' for CRISPR), combines high-throughput sequencing, computational mutation discovery and CRISPR/Cas9-based genome editing^{9, 10}.

To develop this method, we analyzed ispinesib, an inhibitor of kinesin-5 that has entered clinical trials as an anticancer agent (Fig. 1a)^{11–13}. We isolated 12 clones (hereafter referred to as “drug-resistant clones”), that were 70–300-fold less sensitive to ispinesib than the parental cells, (Supplementary Results, Supplementary Fig. 1, Supplementary Table 1). We next analyzed all clones for resistance to five known MDR (multi-drug resistance) substrates. Eight of twelve clones showed minimal to no cross-resistance (Fig. 1b, Supplementary Fig. 2 and 3). Four clones revealed moderate to substantial resistance to the MDR substrates and were not prioritized for further analyses. As expected, ispinesib treatment resulted in monopolar mitotic spindles in parental cells (Fig. 1c)¹⁴. In contrast, bipolar spindles similar to those observed in vehicle-treated controls (Fig. 1d) were observed in ispinesib-treated drug-resistant clones (Fig. 1e). The mitotic indices of ispinesib and nocodazole treated drug-resistant and parental cells were similar (Supplementary Table 4). Together, these data suggest that ispinesib-resistance in these 8 clones is not conferred by indirect mechanisms, such as suppression of the spindle assembly checkpoint or MDR.

Transcriptome sequencing was performed on the ispinesib-resistant clones and parental cells. Known mechanisms of resistance to kinesin-5 inhibition include overexpression of kinesin-12 or centrosome separation secondary to EGFR activation^{15, 16}. No significant differences were observed in the expression of kinesin-12 and EGFR transcripts between ispinesib-resistant clones and the parental cell line (Supplementary Fig. 4). A more extensive analysis indicated that the expression levels of a small number of genes (19 up-regulated and 4 down-regulated) were significantly altered in drug-resistant clones (Supplementary Fig. 5). We cannot exclude the possibility that some of these genes are involved in drug resistance. However, the magnitude of changes and the number of differentially expressed genes was lower than what we have observed in clones resistant to other drugs⁷ and therefore, we did not prioritize analyzing these genes further.

We next focused on identifying genetic mutations that may confer drug resistance. We applied computational analysis to the transcriptome sequencing reads to identify expressed genes in each clone that have mutations that are absent or undetectable in the parental cells⁷. Central to our approach is finding genes that are most frequently mutated in ‘independent’, i.e. least genetically related drug-resistant clones, as these genes are likely to express the drug's direct target⁷. Using methods previously reported the 8 clones were clustered into 5 ‘independent’ groups⁷. Only nine genes were mutated in more than one group (Fig. 2a, Supplementary Tables 5–13). Kinesin-5 was the only gene mutated in more than two groups. In fact, this gene was mutated in each of the 8 drug-resistant clones, and three different mutations were identified (Supplementary Table 13).

In order to analyze whether any one of the identified kinesin-5 mutations is sufficient to confer ispinesib-resistance, we used the CRISPR/Cas9 ‘nickase’ system and homology directed repair (HDR)^{9, 10}. As HDR can be inefficient, selectable markers have been employed to obtain cells with desired mutations^{9, 17}. We postulated that the drug itself could be used to select for genome-edited clones. HeLa cells were transfected with the Cas9 ‘nickase’ and homologous template DNA with or without the kinesin-5 A133P mutation. Wildtype transfectants produced no surviving colonies after drug selection (not shown). In mutant transfectants, mutagenesis of the A133 residue was confirmed using the SURVEYOR mutation detection assay¹⁸ (Supplementary Fig. 6), and Sanger sequencing of the genomic locus (Fig. 2b). We found that the A133P mutation conferred 150-fold resistance to ispinesib (Fig. 2c). This mutation, along with the other two kinesin-5 mutations we identified, map to the protein’s drug-binding pocket (Supplementary Fig. 7). Point mutations (e.g. D130, A133) and deletions (e.g. residues in ‘loop-5’) within this pocket have been shown to confer resistance to ispinesib-analogs *in vitro*¹⁹. Therefore, with these data, we can confirm kinesin-5 to be ispinesib’s direct physiologic target in a human cancer cell line.

We also successfully applied the CRISPR/Cas9 ‘nickase’ system combined with drug selection to introduce point mutations that confer resistance to the proteasome inhibitor Velcade²⁰ (Supplementary Fig. 8) in two cancer cell lines. Together, these data indicate that this genome-editing protocol can overcome a major bottleneck in establishing the ‘genetic’ proof of a drug’s physiological target.

Sequencing data from our ispinesib-resistant clones revealed that the mutant kinesin-5 alleles represent 85 – 100% of the sequencing reads (Supplementary Tables 5–12) in each clone. A similar pattern of mutant kinesin-5 allele expression was observed in the genome-edited, drug-selected HeLa kinesin-5 A133P cells (Supplementary Fig. 9). This near-homozygosity suggests that the wildtype kinesin-5 allele is lost in a large fraction of the resistant cells or that the mutated allele is amplified. These two scenarios are unlikely as kinesin-5 mutations are heterozygous at the DNA level (Fig. 2d) and kinesin-5 transcript levels are slightly decreased in resistant clones compared to parental cells (Supplementary Fig. 10). We propose that wildtype kinesin-5 is silenced by an epigenetic mechanism, e.g. promoter DNA hypermethylation or repressive histone modifications. We reason that since kinesin-5 functions as a homotetramer²¹, cells undergo selective pressure to preferentially express the mutated, drug-resistant allele in order to generate bipolar spindles and complete mitosis. As the chemical inhibitor acting on any motor domain may inhibit activity, only the tetramer comprised of four mutants is likely to be able to confer drug resistance (Supplementary Fig. 11). We propose that such regulation of gene expression to confer drug resistance may also be important for other targets that exist in multiple-copies within multi-protein complexes.

We next used DrugTargetSeqR to examine the mechanisms of action of YM155 (sepantronium bromide), a cytotoxic drug that has entered clinical trials as an anticancer agent²². While the discovery of YM155 was based on its ability to suppress survivin expression, questions have been raised about its mechanism of action²². We selected YM155-resistant clones, analyzed their multi-drug resistance, and sequenced their

transcriptomes (Supplementary Fig. 12). Remarkably, the number of mutations identified in the drug-resistant clones was ~10-fold higher than in the other cases we have analyzed⁷ (see also Supplementary Tables 5–12). These data indicate that YM155 is likely to be a mutagenic agent, consistent with YM155's chemical structure which suggests it may intercalate DNA and other reports that YM155 treatment activates the DNA damage response²³. While analyses of genetic mutations do not reveal a specific resistance mechanism, the gene expression data indicates that resistance to YM155 is likely due to reduced cell proliferation (Supplementary Fig. 9d). We have also applied our methodology to multi-targeted agents (e.g. sorafenib) and have had difficulty selecting clones resistant to the drug, but not other MDR substrates, likely due to a low probability that a single cell could acquire 2 (or more) resistance-conferring mutations simultaneously without a substantial loss in fitness.

Overall, our findings indicate that DrugTargetSeqR is an effective method for identifying the targets of cytotoxic drugs (Fig. 2e). The CRISPR/Cas9-based genome editing step has several advantages, as mutations can be engineered in to the endogenous locus, and interaction between multiple genetic alterations can be analyzed. Further, when two drugs are effective in combination and resistant mutations to one are known, we can readily introduce these mutations and analyze the second agent's target and resistance mechanisms. At this stage we favor the use of transcriptome sequencing, as most drugs target expressed proteins, and the sequencing data include gene expression levels and mutations. However, other strategies such as exome-capture followed by sequencing may be used to detect copy number alterations and mutations in genes expressed at low levels²⁴. We also believe that compounds that target regulatory sequences or noncoding transcripts could be analyzed using DrugTargetSeqR. Specifically, observed changes in gene expression could be followed by targeted sequencing of specific promoters and regulatory regions.

We are optimistic that we can further improve the general applicability of DrugTargetSeqR. To analyze mechanisms of action of non-cytotoxic agents, drug-resistant clones could be selected using reporter gene expression or a phenotype that can be readily measured for a few or single cells, e.g. by high-throughput microscopy. Furthermore, the use of suspension cell lines in place of adherent lines may allow for high-throughput analysis of drug targets, since the selection and expansion of drug resistant clones could be carried out by dilution, a step that is more readily compatible with automated liquid transfers.

Online Methods

Chemical compounds

Ispinesib (S1452) and mitoxantrone (S2485) were purchased from Selleck Chemicals. Nocodazole (74151), paclitaxel (T7402), and vinblastine (V-1377) were purchased from Sigma. Irinotecan was purchased from LC Laboratories (I-4122). All compounds were dissolved in dimethylsulphoxide (DMSO).

Cell Biology

For isolation of drug-resistant clones, we chose the HCT116 cell line as it is known to be mismatch-repair deficient and hence genetically unstable, and is known to express low

levels of drug-efflux pumps responsible for multidrug resistance (MDR)⁷, a common mechanism of drug resistance in human cancer cells. However, prior work has revealed that under drug selection, even HCT116 cells may be selected for high MDR expression⁷. In order to test whether any single mutation could confer resistance, the comparatively genetically-stable, mismatch-repair intact cell line HeLa was used for CRISPR-based genome editing. The HCT116 cell line was purchased from ATCC. HeLa and HEK293E were kind gifts from Dr. Charles Sawyers, MSKCC. HCT-116 cells and clonal lines were cultured in McCoy's 5A medium (Invitrogen), while HeLa and HEK293E were cultured in Dulbecco's Modified Eagle's medium (Invitrogen). All cultures were supplemented with 10% FBS (Atlanta Biologicals) and penicillin-streptomycin (100 U/ml and 100 ug/ml, respectively, Invitrogen) and grown at 37°C in a humidified chamber with 5% CO₂. HeLa and HEK293E were also supplemented with 2 mM L-glutamine (Invitrogen).

Selection of resistant clones

Resistant clones were generated as previously described⁷. Briefly, 0.5 – 1.0 × 10⁶ HCT116 cells were plated in 10 cm culture dishes with media containing ispinesib at a final concentration of 50 – 125 nM and 0.1% DMSO. Media with compound was exchanged every three days for two to four weeks. Most cells did not survive, but a few per plate grew into colonies. Typically fewer than 10 colonies were found on each plate. Colonies were picked by ring cloning and transferred to a new plate where they were maintained in media containing drug at the same concentration as the selections.

Cell proliferation assays

In order to quantify cell growth in the presence of drug, cells (2000 cells in 100 µl of media per well) were plated in flat-bottomed 96-well plates and treated with 4 or 8 doses of a serial dilution of the compound of interest. Each condition was plated in triplicate. After three days, cell proliferation was determined using a WST1 assay (Millipore) according to the manufacturer's instructions. Absorbance was read at 440 nm and 690 nm using a BioTek Synergy Neo HTS Plate Reader. Data were used to generate dose response curves as described below.

Dose Response Analysis

For each experiment, cellular proliferation (mean absorbance of 3 reads) and error bars (standard deviation) versus concentration of drug were plotted. For each experiment, data were fit using Eq. 1 to find the LD₅₀. Three independent experiments were performed for each condition. The mean LD₅₀ and standard deviation of 3 independent experiments are shown in Supplementary Tables 1, 2, and 3.

$$y = \min + \frac{(\max - \min)}{1 + 10^{\log EC_{50} - x}} \quad \text{Eq. 1}$$

Immunofluorescence

All experiments were performed on a Zeiss Axioplan2 microscope (Carl Zeiss MicroImaging), with a 40x objective (Plan Neo, NA 0.75) and DeltaVision Image Restoration Microscope (Applied Precision). HCT116 cells were plated on glass coverslips (Fisher Scientific) in 6-well dishes 24 hours before fixation. Cells were exposed to DMSO only (vehicle control), ispinesib (50 and 100 nM) for 4 hours, or 50 ng/mL (166 nM) nocodazole for 14 hours at 37 °C in complete media. Cells were fixed for 10 min at 37°C in fix solution (4% formaldehyde, 0.2% Triton X-100, 10 mM EGTA, 1 mM MgCl₂, 100 mM PIPES pH 6.8). Coverslips were washed 3 times with TBS-tx (TBS + 0.1% Triton X-100), blocked with AbDil (2% BSA in TBS-tx buffer) and incubated for 1 hr at room temperature with FITC-conjugated mouse anti-tubulin monoclonal antibody (Sigma # F2168; 1:2000 dilution in AbDil). Coverslips were washed three times in TBS-tx, and DNA was stained with Hoechst 33342 (Sigma; 1:10,000). Coverslips were mounted in 0.5% p-phenylenediamine (Sigma) in 20 mM Tris, at pH 8.8, with 90% glycerol and sealed with nail polish.

Nucleic Acid Purification, PCR, and Sanger Sequencing

Total RNA was isolated from cells using the RNeasy Mini Kit (Qiagen) according to the manufacturer's instructions. Genomic DNA was isolated from cells using the DNeasy Mini Kit (Qiagen) according to manufacturer's instructions. PCR amplification of the genomic locus for vector construction, SURVEYOR assay, and sequencing reactions was performed using AccuPrime™ Pfx DNA Polymerase according to manufacturer's recommendation.

Vector construction

The SpCas9n "nickase" targeting vector pX335 [Plasmid 42335: pX335-U6-Chimeric_BB-CBh-hSpCas9n(D10A)] was kindly provided by Dr. Luciano Marraffini (Rockefeller University). Vector was digested using BbsI (NEB), and a pair of annealed oligos were ligated into the guide RNA construct.

The synthetic guide RNA targeting kinesin-5 exon 5 was generated using oligos 5'-caccttcagtc aaagtgtctctgt-3' and 5'-aaacacagagacactttgactgaa-3'. The synthetic guide RNA targeting psmb5 was generated using oligos 5'-caccaccatggctgggggcgcag-3' and 5'-aaactgcgccccagccatggtg-3'.

Template DNA containing the single base pair change uncovered in our screen (kinesin-5 A133P) was generated using PCR-amplification of a pBlueScript vector containing the desired point mutation flanked by 1kb homology arms to generate a 2kb template for Homology Directed Repair. Point mutants were generated using Quikchange site-directed mutagenesis (Stratagene) of pBlueScript engineered to contain the 2 kb fragment of the genomic sequence flanking the desired mutation. Wildtype genomic DNA inserts were amplified from parental cells, and blunt ligated in to EcoRV-digested pBluescript. All constructs were sequence verified using Sanger sequencing in both directions and compared to reference sequence GRCh37.p13. PCR amplified template was gel purified before use in transfection. For amplification of the genomic region of kinesin-5 exon 5, genomic DNA from parental cells was amplified using primers 5'-taaagtgatgggtcccactg-3' and 5'-

tgaccatgtctcccacact -3'. For amplification of the genomic region of psmb5, the primers 5'-cagtagccacaagccacaca-3' and 5'-aggcctcttggtgattcc-3' were used. Site-directed mutagenesis using Quikchange employed the following primers: kinesin-5 A133P was mutagenized using primers: 5'-taatttcaggatcccttgctgtataattccac -3' and 5'-gtacgtggaattataaccaggcaaggatcctg-3'. Psmb5 was mutagenized using 5'-cgccccagccacgggtgccaagcagg-3' and 5'-cctgcttgccaccgtggctgggggcg-3' (M104V) and 5'-accatgctggggcacagcggattgcagct-3' and 5'-aagctgcaatccgctgtgccccagccatggt-3' (A108T).

Transfection and Selection

Cells were seeded onto 12-well plates (BD Falcon) at a density of 400,000 cells/well, 24 hours prior to transfection. Cells were transfected using FuGene6 transfection agent at 80%–90% confluency following the manufacturer's protocol. A total of 1000ng pX335 Cas9 plasmid and 1000 ng of HDR template PCR product was transfected to each well. Cells were incubated at 37°C for 48 hours post-transfection prior to drug exposure, at which point they were expanded to 6cm dishes in ispinesib 10 nM. Transfected cells were maintained in escalating doses of drug to a final concentration of 100nM for 10 days, during which time most cells died. Media with drug was exchanged every three days. Cells were split, expanded, and harvested for genomic DNA as described above in Nucleic Acid Purification.

SURVEYOR Nuclease Assay for Genome Modification

A 390 bp genomic region flanking the CRISPR target site for each gene was PCR amplified using primers listed above and gel purified using QiaQuick Spin Column (QIAGEN) following the manufacturer's protocol. 400 ng total of the purified PCR products were eluted using 10mM Tris-HCl pH 8.8, 15 mM MgCl₂, 50 mM KCl to a final volume of 20 µl and were subjected to a reannealing process to enable heteroduplex formation: 95°C for 10 min; 95°C to 85°C ramping at -2°C/s; 85°C to 25°C at -0.25°C/s; and 25°C hold for 1 min. After reannealing, products were treated with SURVEYOR nuclease and SURVEYOR enhancer S (Transgenomics) following the manufacturer's protocol and were analyzed on 4%–20% Novex TBE polyacrylamide gels (Life Technologies). Gels were stained with EtBr and imaged using ultraviolet light.

RNA-Seq library construction and sequencing

Library construction for RNA-Seq was performed as previously described⁷, following standard Illumina protocols using Illumina reagents by the Weill Cornell Genomics Core Facility. Sequencing was performed using the Illumina HiSeq2500 using SR 51bp. Three samples were run per lane.

Overall bioinformatics strategy

Identification of reads mapping to exons and across known exon junctions was performed as previously described⁷. All mapped reads were remapped to the hg18 reference human genome using custom programs based on the June 2010 RefSeq gene annotation. Mutation detection, clone clustering, and merging was performed as previously described⁷, with one modification. In previous work, we had initially reasoned that a two-hit mutation involving the same exact nucleotide (mutation of two alleles) would be unlikely, and were therefore

using a filter eliminating homozygous or near-homozygous mutations. We have removed this filter from the current analysis and recommend not using that filter in light of the results seen here. (Removing the filter had no influence on the previously published results.) All bioinformatics protocols can be found at <http://icb.med.cornell.edu/wiki/index.php/Elementolab/TargetID>.

Supplementary Material

Refer to Web version on PubMed Central for supplementary material.

Acknowledgments

We are grateful to the NIH (GM98579, PI TMK) and Starr Cancer Consortium (I6-A618 to OE and TMK). CK was supported by the Louis and Rachel Rudin Foundation and a Medical Scientist Training Program grant (NIH/NIGMS T32GM007739) to the Weill Cornell/Rockefeller/Sloan-Kettering Tri-Institutional MDPHD Program.

References

1. Schenone M, Dancik V, Wagner BK, Clemons PA. Target identification and mechanism of action in chemical biology and drug discovery. *Nature chemical biology*. 2013; 9:232–240. [PubMed: 23508189]
2. Titov DV, Liu JO. Identification and validation of protein targets of bioactive small molecules. *Bioorganic & medicinal chemistry*. 2012; 20:1902–1909. [PubMed: 22226983]
3. Bassik MC, et al. A systematic mammalian genetic interaction map reveals pathways underlying ricin susceptibility. *Cell*. 2013; 152:909–922. [PubMed: 23394947]
4. Shalem O, et al. Genome-scale CRISPR-Cas9 knockout screening in human cells. *Science*. 2014; 343:84–87. [PubMed: 24336571]
5. Wang T, Wei JJ, Sabatini DM, Lander ES. Genetic screens in human cells using the CRISPR-Cas9 system. *Science*. 2014; 343:80–84. [PubMed: 24336569]
6. Weiss WA, Taylor SS, Shokat KM. Recognizing and exploiting differences between RNAi and small-molecule inhibitors. *Nature chemical biology*. 2007; 3:739–744. [PubMed: 18007642]
7. Wacker SA, Houghtaling BR, Elemento O, Kapoor TM. Using transcriptome sequencing to identify mechanisms of drug action and resistance. *Nature chemical biology*. 2012; 8:235–237. [PubMed: 22327403]
8. Stratton MR, Campbell PJ, Futreal PA. The cancer genome. *Nature*. 2009; 458:719–724. [PubMed: 19360079]
9. Cong L, et al. Multiplex genome engineering using CRISPR/Cas systems. *Science*. 2013; 339:819–823. [PubMed: 23287718]
10. Mali P, et al. RNA-guided human genome engineering via Cas9. *Science*. 2013; 339:823–826. [PubMed: 23287722]
11. Bergnes G, Brejc K, Belmont L. Mitotic kinesins: prospects for antimetabolic drug discovery. *Current topics in medicinal chemistry*. 2005; 5:127–145. [PubMed: 15853642]
12. Rath O, Kozielski F. Kinesins and cancer. *Nature reviews Cancer*. 2012; 12:527–539. [PubMed: 22825217]
13. Sakowicz R, et al. Antitumor activity of a kinesin inhibitor. *Cancer research*. 2004; 64:3276–3280. [PubMed: 15126370]
14. Mayer TU, et al. Small molecule inhibitor of mitotic spindle bipolarity identified in a phenotype-based screen. *Science*. 1999; 286:971–974. [PubMed: 10542155]
15. Mardin BR, et al. EGF-induced centrosome separation promotes mitotic progression and cell survival. *Developmental cell*. 2013; 25:229–240. [PubMed: 23643362]
16. Sturgill EG, Ohi R. Kinesin-12 differentially affects spindle assembly depending on its microtubule substrate. *Current biology: CB*. 2013; 23:1280–1290. [PubMed: 23791727]

17. Bassett AR, Tibbit C, Ponting CP, Liu JL. Mutagenesis and homologous recombination in *Drosophila* cell lines using CRISPR/Cas9. *Biology open*. 2014; 3:42–49. [PubMed: 24326186]
18. Guschin DY, et al. A rapid and general assay for monitoring endogenous gene modification. *Methods in molecular biology*. 2010; 649:247–256. [PubMed: 20680839]
19. Talapatra SK, Anthony NG, Mackay SP, Kozielski F. Mitotic kinesin Eg5 overcomes inhibition to the phase I/II clinical candidate SB743921 by an allosteric resistance mechanism. *Journal of medicinal chemistry*. 2013; 56:6317–6329. [PubMed: 23875972]
20. Adams J. The development of proteasome inhibitors as anticancer drugs. *Cancer cell*. 2004; 5:417–421. [PubMed: 15144949]
21. Cole DG, Saxton WM, Sheehan KB, Scholey JM. A “slow” homotetrameric kinesin-related motor protein purified from *Drosophila* embryos. *The Journal of biological chemistry*. 1994; 269:22913–22916. [PubMed: 8083185]
22. Holmes D. Cancer drug’s survivin suppression called into question. *Nature medicine*. 2012; 18:842–843.
23. Glaros TG, et al. The “survivin suppressants” NSC 80467 and YM155 induce a DNA damage response. *Cancer chemotherapy and pharmacology*. 2012; 70:207–212. [PubMed: 22526412]
24. Shendure J, Ji H. Next-generation DNA sequencing. *Nature biotechnology*. 2008; 26:1135–1145.

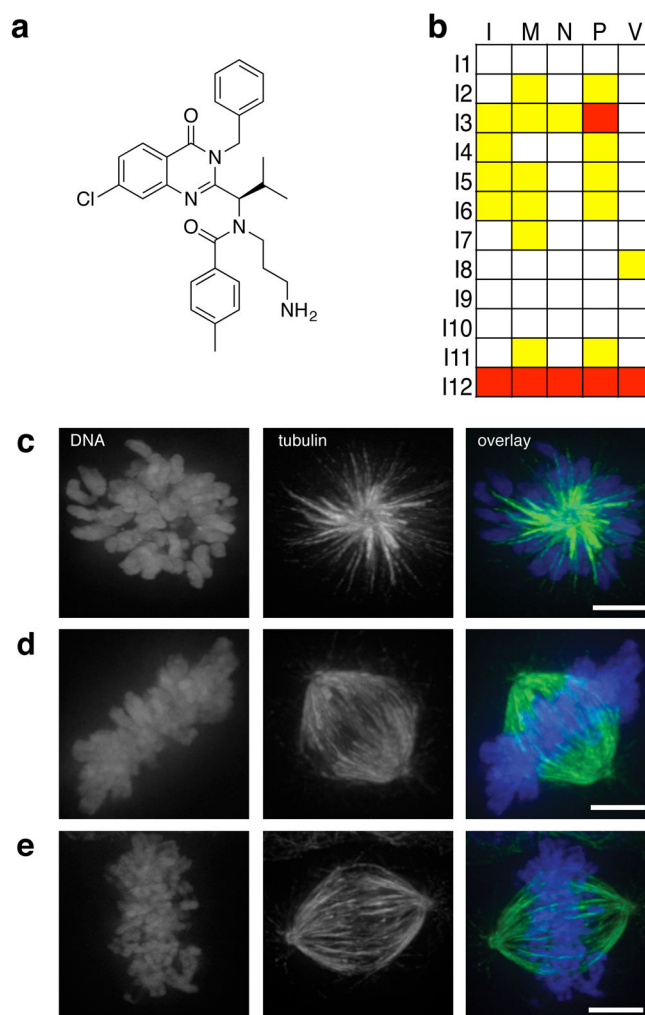


Figure 1. Characterization of ispinesib resistant clones

(a) Structure of kinesin-5 inhibitor ispinesib. (b) Comparative analysis of twelve ispinesib-resistant clones (I1 – I12) against five MDR substrates: irinotecan (I), mitoxantrone (M), nocodazole (N), paclitaxel (P) and vinblastine (V). White box: similar activity as parental cells, Yellow box: moderate reduction in sensitivity, Red box: substantial reduction in sensitivity. Representative dose response curves and LD₅₀ values are shown in Supplementary Fig. 2 and Supplementary Table 2. (c – d): Analysis of mitotic spindles in parental and ispinesib-resistant cells. Maximum intensity projections of DNA (blue) and tubulin (green), and an overlay of the two images are shown. (c,d) Parental HCT116 cells treated with ispinesib (50 nM, 4hrs) (c) or vehicle control (d) were fixed and processed for immunofluorescence. (e) Ispinesib-resistant Clone I7 treated with ispinesib (50 nM, 4hrs) was fixed and processed for immunofluorescence. Scale bar: 5 μ m.

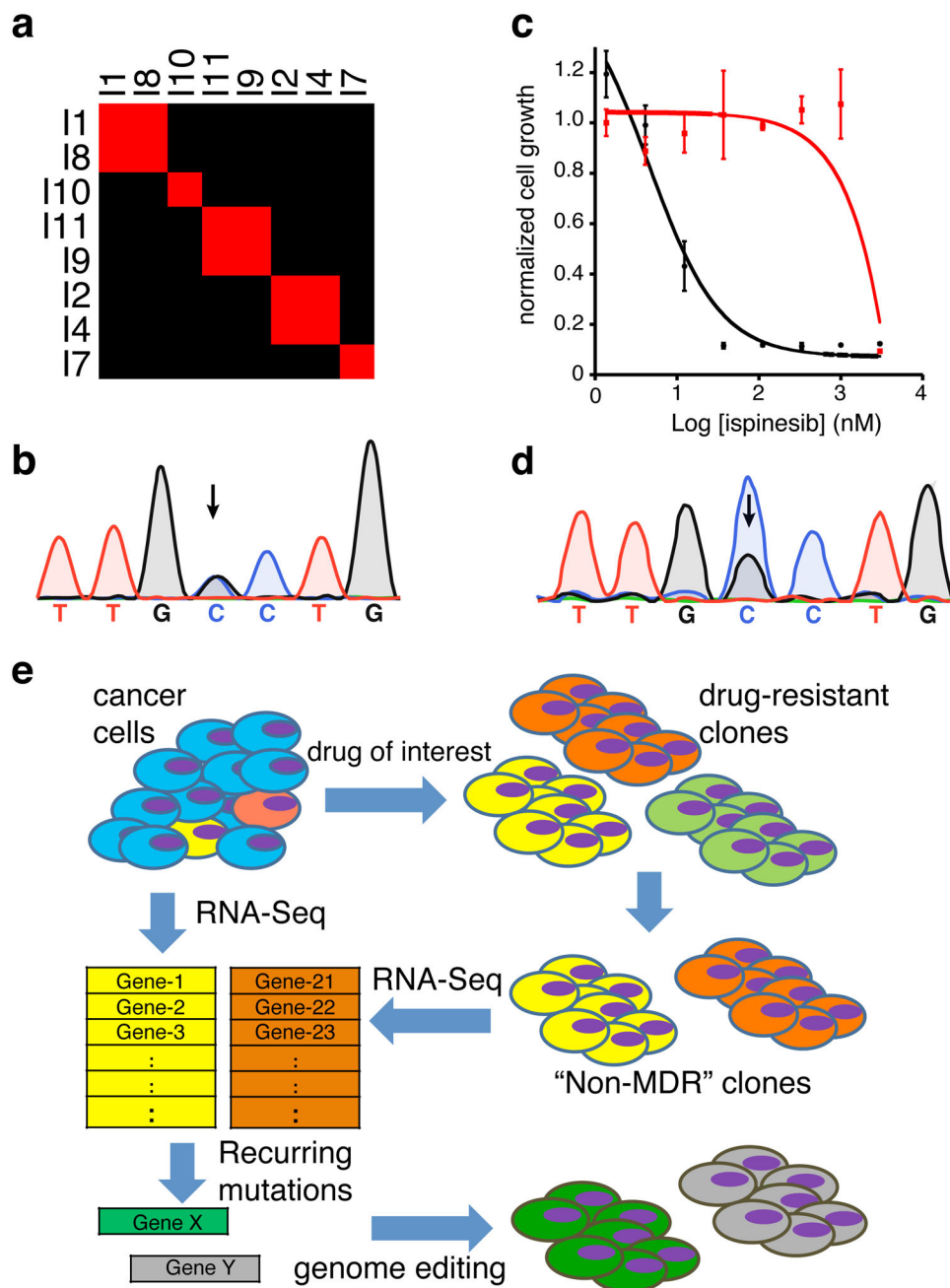


Figure 2. Identification of high-frequency resistance-conferring mutations

(a) Hypergeometric distribution-based clustering (red = high; black = low similarity) of 8 clones processed for RNA-Seq. Clones collapsed to 5 independent groups. (b, d) Sanger sequencing traces of DNA for the genomic locus of the kinesin-5 A133P mutation in genome-edited HeLa cells (b) or HCT116 ispinesib-resistant clone I11 (d) after selection in 100nM ispinesib. Arrow indicates site of mutation. (c) LD50 values measured for parental HeLa (black) and genome-edited A133P mutation-carrying cells (red). LD50 values: 2.3 – 6.4 nM (parental), >1000 nM (HeLa A133P). Error bars (s.d.) were generated from 3 Wst1 assays done in parallel. Two independent sets of experiments were performed. (e) Schematic

highlighting key steps of DrugTargetSeqR. Genetically heterogenous cancer cells are treated with the drug of interest, resistant clones are isolated, and those resistant to MDR substrates excluded. The remaining clones along with the parental cells are processed for RNA-Seq. Mutations present in each drug-resistant clone, but absent in the parental (untreated) cell, are analyzed to identify genes that are frequently mutated in independent groups. CRISPR/Cas9 and drug-based selection is then used to isolate otherwise drug sensitive cells with these mutations.

Author Manuscript

Author Manuscript

Author Manuscript

Author Manuscript